SWS FRINGES AND MODELS

Do Kester[1], Douwe Beintema[1], Dieter Lutz[2]

[1] *Space Research Organization of the Netherlands, Postbus 800, NL-9700 AV Groningen, the Netherlands*
[2] *Max Planck Institut für Extraterrestrische Physik, Giessenbachstrasse 1, D-85748 Garching, Germany*

ABSTRACT

Fringes are present in all grating bands of the SWS instrument. Here we describe how they occur and what can be done about them. Some tentative conclusions are drawn for future missions.

Key words: ISO, SWS, Data Analysis, Fringes

1. Introduction

All SWS bands show to some extent fringes. Fringes originate on parallel plane surfaces in the light path which act as Fabry-Pérot etalons. Plane parallel surfaces at a distance of a few mm up to a few cm are perfect to cause FP effects in the infra red wavelength range. It is not surprising that they occur in the SWS spectrometer at almost all wavelengths. It is assumed that etalons are formed inside filters, on plane mirrors and, most conspicuously in band 3, in the BIBIB detectors themselves. And of course in combinations of all of them, resulting in a sometimes wild fringe pattern. Every reflecting surface which is added to the light path can add N-1 extra fringe components disregarding all the overtone options.

Most of the observed fringe pattern disappears in the calibration process where the observation is divided by a similarly fringed relative spectral response function (RSRF). Still some residual fringing remains in the calibrated spectrum. Its exact pattern is presumably determined by the exact location of the source in the slit. When shifting from one spot (well) within the slit to another, it is observed that the fringe pattern does not shift as a whole, but different components of the fringe pattern shift by different amounts. The result is a completely changed fringe pattern which cannot be matched by one single RSRF. Another cause of extra fringing is found in the combination of the size of the observed object and the speed at which its spectrum is scanned. This combination determines the smoothing in the spectrum. Ideally the RSRF should match exactly the smoothness of the observation. Which is almost never the case. The RSRF was observed at full spectral resolution during ground tests using a black body temperature source which filled the slit completely. So for AOT2 and 6, and for slow AOT1s we have an RSRF where the fringes are not sharp enough and for fast AOT1s the RSRF is not smooth enough. In the pipeline processing we try to remedy this by smoothing or peaking up the RSRF according to the speed of the observation. The three reasons mentioned above (location, speed and extent) can cause a *residual* fringe pattern in some AOT-bands of up to 10%.

2. Modeling

One of the first efforts to model the fringes was to apply rigorous optical theory (Haser, 1996). For a simple etalon we can write the intensity I as

$$I = \frac{T^2}{(1-R)^2}[1 + \frac{4R}{(1-R)^2}\sin^2(2\pi DK + \varphi)]^{-1} \quad (1)$$

Here T is the transmission of the etalon surfaces, R is the reflectivity of the surfaces, D is the effective thickness of the etalon, K is the wavenumber and φ is the phase shift at reflection. This setup could claim some successes for simple fringe patterns in the uncalibrated data, not yet 'corrected' by division of the RSRF. But the full blown SWS fringe patterns with dozens of components which moreover were partly corrected by the RSRF, turned out to be much too complicated.

After division by the RSRF we can assume that the *residual* fringes are small in amplitude. With this assumption and after subtraction of a smoothed background intensity, we can approximate equation 1 and obtain a much simpler one.

$$I = \alpha\cos(4\pi DK + \varphi) \quad (2)$$

The constant α is a rather complex combination of T and R. In a fringe pattern all the components are acting independently so we can simply add a number of these fringes together.

$$I = \sum_{n=1}^{N} \alpha_n \cos(4\pi D_n K + \varphi_n) \quad (3)$$

Each fringe component is characterized by 3 parameters: the effective distance D, the amplitude α and the phase φ. Equivalently we can rewrite this in a computationally more handy form.

$$I = \sum_{n=1}^{N} A_n \cos(4\pi D_n K) + B_n \sin(4\pi D_n K) \quad (4)$$

where A and B are constants. The effective distance D is also referred to as the 'cycle' of the fringe.

3. Removal

Fringes are removed by first modeling them and then dividing out the model fringe pattern. The modeling is done per AOT band, defined by aperture, order and detector band as each AOT band follows a different light path through the instrument. The fringes are modeled on data where the smooth background has been removed. Determining the smooth background is somewhat of an art; it is one of the reasons that fringe removal cannot be done in a completely automated fashion within the pipeline.

Due to their linear appearance in expression 4, the constants A and B can be calculated quite easily, provided that D is known. So the problem is down to finding D and finding out how many fringe components, N, there are.

When N components have been found, finding a possible next component D_n entails a linear search for the minimum in

$$\chi^2 = \sum (y_k - I_N - A_n \cos(4\pi D_n K) - B_n \sin(4\pi D_n K))^2$$

where y_k is the fringed data with their smooth background subtracted. We calculate χ^2 for all values of D within the range where the fringe cycles are known to occur, see section 4. At the minimum i.e. for the best choice of D_n we want to determine whether this newly found fringe component is a valid one. We calculate the evidence for this model including the new component. The evidence measures the odds between two models by combining the likelihood, i.e. the goodness of the fit, with the so-called Occam factor. This Occam factor penalizes overly complex but well fitting models. For details see eg. (MacKay, 1992) or (Sivia, 1996). If the evidence for this model is larger than for the previous one, without the component, then we keep the component and start searching for another one. When the evidence is less for this model than for the previous one, we reject the component and stop the procedure. The same procedure can be used to conclude that there are no fringes at all in some bands.

Within SIA and OSIA[1] the ideas expounded here are implemented in the program FRINGES. It can handle both SPDs and AARs —actually it will do RSRFs too— and it will remove (residual) fringes in a completely automated way. Within ISAP[2] these ideas are partially implemented in the program AARFRINGE.

[1] The Observers SWS Interactive Analysis (OSIA) package can be downloaded from http://sws.ster.kuleuven.ac.be. It is a package for SWS (post-AAR) processing using IDL v5.3.

[2] The ISO Spectral Analysis Package (ISAP) can be downloaded from http://www.mpe.mpg.de/ISO/isosdc.html.

band	D mm	range of D mm	RSRF %	Residual %	AOT NR
1A	4.20	4.1-4.3	-	8	6,2
1B	4.30	4.2-4.4	-	3	6,2
1D	4.45	4.3-4.5	2	5	6,2
1E	4.58	4.4-4.6	-	1	6,2
2A	4.43	4.4-4.6	1	2	6,2
	0.89	0.8-0.9	0.5	-	
	2.39	2.3-2.4	0.3	-	
2B	4.50	4.4-4.7	2	1	6,2
	0.89	0.8-0.9	0.6	-	
2C	5.86	5.6-6.1	4	4	all
	0.89	0.8-0.9	2	-	
3A	3.37+3.25	3.2-3.4	25	5	all
	5.26+5.72	5.0-6.0	10	5	
3C	3.25+3.38	3.2-3.4	17	4	all
3D	3.25	3.2-3.4	17	2	all
3E	3.28	3.2-3.4	19	2	all
4	13.25	13.2-13.3	0.2	-	-
4A	5.27+5.73	5.0-6.0	10	3	all
4C	6.67	6.5-6.8	1	-	all
4D	-	-	-	-	-

Table 1. Main fringe components per AOT band. The second column gives the effective thickness for the main components. Sometimes there is more than one component. These are listed separately when the components are quite distinct. Column 4 and 5 list the compound amplitude in percent, of the fringe components in resp. the RSRF and of the residual fringes in some observations on point sources. The last column list the AOT numbers where these residual fringes might be found.

4. RSRF

As the residual fringes in a spectrum are caused by various kinds of mismatches of the RSRF, the cycles of the fringe components can only be the ones which are already in the RSRF, or rather which *should* have been in the RSRF. Particularly in band 1 we observe in AOT6s i.e in full resolution mode, on some point sources high frequency fringes that are *not* seen in the RSRF. These fringes have only 4 scanner steps on one complete cycle. The full illumination of the slit while measuring the RSRF in the laboratory washed out all this fringing.

So with some precaution we can use the RSRF to find which cycles are present in the different AOTbands. In table 1 we list per AOT band where the main fringe components are and what their compound amplitude is in percent. In some bands there are hardly any fringes in the RSRF to be found. To check whether there are no fringes at all, we also looked at AOT6 or AOT1 speed 4 observations of point sources to find the residual fringes in there.

Comparing the amplitude of the fringes in the RSRF with *residual* amplitudes in AOT 6 observations (on α Lyr) we see that in band 1 there are clearly fringes lacking in the RSRF. All fringes in band 1 are very narrow. They can only be seen in point sources at the full resolution. In band

2 we see different sets of fringes, from very low frequency (effective thickness of 0.9) to rather high frequency. The low frequency stuff has completely disappeared after division by the RSRF. So we do not see it in the AOT 6. The high frequency stuff is still present in the residuals with the same amplitude as it had in the RSRF. Obviously, division by the RSRF has improved the situation, but it has not eliminated all.

For band 3 and 4 we compare the RSRF fringes with the residuals in an AOT 1 speed 4 observation (of K3-50). In band 3 division by the RSRF reduces the amount of fringing from some 20 % to a few precent. It is present in all AOTs. For that reason fringes were for a long time regarded mainly as a problem in band 3. One set of fringes with a thickness of about 3.3 mm is present in all AOT-bands related to the Si:As detectors. This set is deemed to be caused by the BIBIB detectors themselves. Another set at 5.26 mm present in band 3A is also seen in the 'off-band' 4A. It may be cause by a resonance in the Reststrahlen filter in aperture 1. All in all the fringe system in AOT band 3A is by far the most complicated one. Even when looking at residual fringes we can easily detect more than a dozen.

In the official band 4 we can detect in the RSRF some high frequency fringes at a very small amplitude. As far as we know they have never been reported in real observations. High noise in the observations probably masks these fringes.

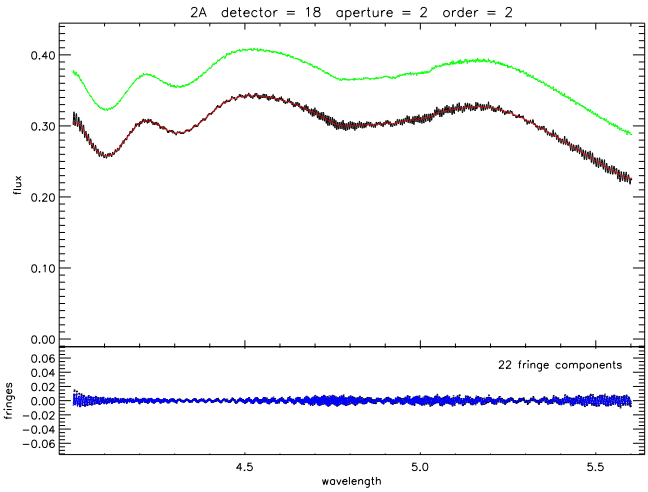

Figure 1. In the upper panel we see the original RSRF in black and the smooth background in red. The difference between these two is plotted in the lower panel in black. To this data the fringe components are fitted; 22 components were found. This fringe pattern is plotted in blue. In the upper panel again in green and shifted somewhat for clarity, is the RSRF with the fringe pattern subtracted.

5. Examples

In this section we give 3 examples of defringing, one on an RSRF, one on an AAR, and one on an SPD; each in a different AOT band. In all cases we used the OSIA program FRINGES in its automatic mode to defringe.

As a first example we present the fringes in the RSRF of band 2A, for one detector only in figure 1. The fringes are small in amplitude and 3 distinct sets of fringes are found (see also figure 2 and table 1). Most of the 'noise' in the RSRF can actually be modeled as fringes. We could determine 22 components, ranging from an amplitude of 0.7 % down to less than 0.1 %.

We present another view on the same data set, the RSRF of band 2A, in figure 2. Here the various fringe components are displayed and also the amount of noise reduction their removal might impose.

The second example is an AOT6 observation of α Lyr presented in figure 3. Here we used an (unrebinned) AAR. In band 1A we find 12 fringe components which are not present in the RSRF. Nonetheless they are undeniably present. In amplitude they range from 3 % down to 0.1 %. We combined all detector data in band 1A. These fringes are so narrow that they can only be found at full resolution in good quality data. Note that the green, defringed

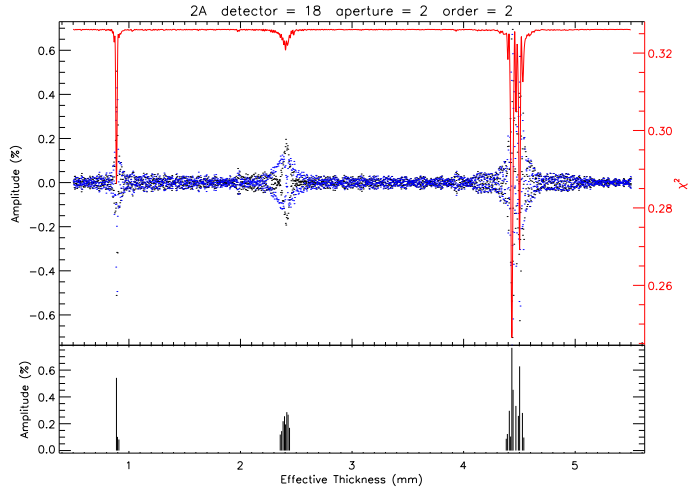

Figure 2. The amplitude of fringe components in the RSRF of band 2A plotted against effective thickness. In the lower panel the amplitude of the 22 fringe components is displayed as a function of separation between the reflecting surfaces. In the upper panel is the situation before any fringe removal. Black and blue display the amplitudes of the cosines and sines as they are found for the various values of the thickness. In red is the value of χ^2.

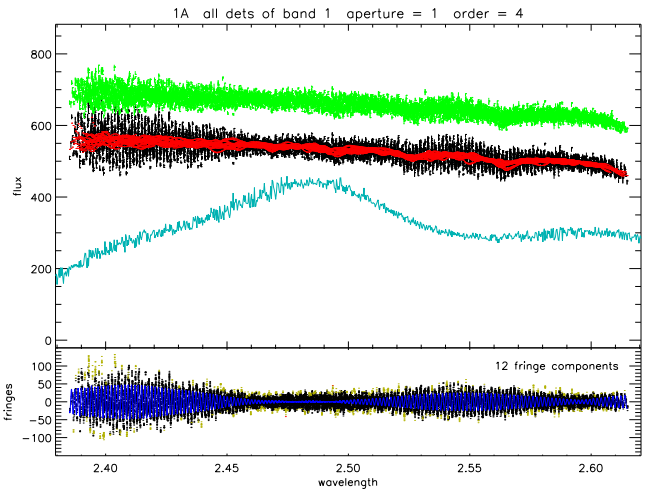

Figure 3. This figure is similar in layout to figure 1. The only extra feature is the (scaled) RSRF in blue-green. It is displayed for comparison. Actually none of the fringes present in the observation can be found in the RSRF.

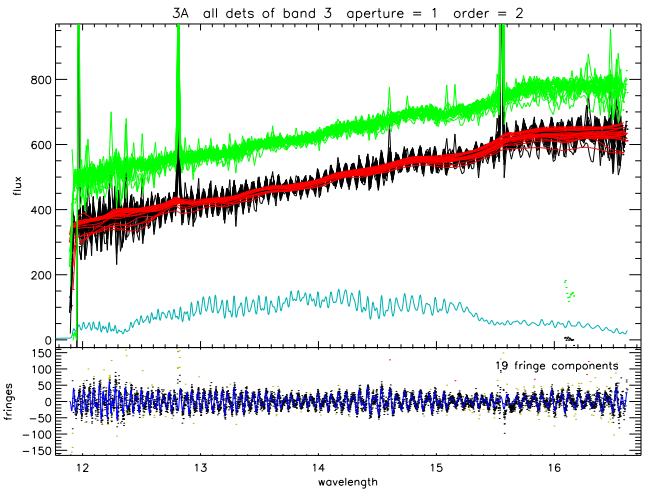

Figure 4. In this figure the layout is similar to the on in figure 3. Note how similar in the details the extracted residual fringe pattern is to that of the RSRF.

spectrum in figure 3 seems noisier than it actually is because we did not do any flatfielding; all detectors are still at a slightly different level as can also be gleaned from the smoothed backgrounds, displayed in red.

For our third example of the removal of residual fringes we took an AOT1 speed 4 observation of K3-50. The star α Lyr has not enough flux at the longer wavelengths, so we chose an HII-region. We had the SPD of K3-50 flux calibrated. In this process the observed fringes should have been removed by division by the RSRF. Still we see some remaining fringes, particularly in band 3. Here we present in figure 4 band 3A fringes, the most complex fringe pattern present in SWS data. As in figure 3 we took all detectors together to improve the fringe signal for detection. It turns out that the residual fringes of all detectors show mostly the same behaviour. 19 Fringe components could be detected in this particular source, ranging in amplitude from 4.1 % down to 0.3 %. Not only do all detectors show the same residual fringe behaviour, also the detailed correspondence between the RSRF and the residual fringe pattern is very conspicuous, and reassuring. It increases the confidence that the defringing removed RSRF fringes only and that it is not eating into true observed flux. The same last remark as in the α Lyr case, holds here too. The green defringed spectrum seems noisier in figure 4 than it really is due to the lack of flatfielding.

6. Conclusions.

The conclusions are given here in the form of 'lessons learned'.

- Fringes are everywhere. SWS-like instruments for detection of infrared or submm spectra are of just the right size to make them effective fringe detectors. Every two plane parallel surfaces a few mm apart give rise to a nice set of fringes. During the design special attention should be given to actively *preventing* fringes e.g. by using wedged filters.
- The RSRF should be measured in the laboratory using a point source simulator.
- Fringes can be detected automatically down to 0.1 % of the amplitude in good quality data.

REFERENCES

Haser, L. "Fringe Modeling in ISO SWS Band 3", Technical Note. MaxPlanck Institut fuer Extraterrestrische Physik, Garching. 3 Dec 1996.

MacKay, D. "Bayesian Interpolation", in *Maximum Entropy and Bayesian Methods*, Eds: C. Smith et al. pp. 39-66. Kluwer, Dordrecht. 1992.

Sivia, D.S. "Data Analysis, A Bayesian Tutorial.", Oxford University Press, 1996.